OBJECTIVE QUALITY ASSESSMENT AND OPTIMIZATION FOR HIGH DYNAMIC RANGE IMAGE TONE MAPPING

V.PHANI BHUSHAN,
Associate Professor, ECE Dept., PBR VITS, Kavali, Nellore (Dt.), AP, INDIA

B.SRAVANI,
PG Scholar, DSCE, ECE Dept., PBR VITS, Kavali, Nellore (Dt.), AP, INDIA

ABSTRACT

Tone mapping operators aim to compress high dynamic range (HDR) images to low dynamic range ones so as to visualize HDR images on standard displays. Most existing works were demonstrated on specific examples without being thoroughly tested on well- established and subject-validated image quality assessment models. A recent tone mapped image quality index (TMQI) made the first attempt on objective quality assessment of tone mapped images. TMQI consists of two fundamental building blocks: structural fidelity and statistical naturalness. In this thesis, we propose an enhanced tone mapped image quality index (eTMQI) by 1) constructing an improved nonlinear mapping function to better account for the local contrast visibility of HDR images and 2) developing an image dependent statistical naturalness model to quantify the unnaturalness of tone mapped images based on a subjective study. The advantages of this algorithm are twofold: 1) eTMQI and TMQI can be compared in a more straightforward way; 2) better qualitytone mapped images can be automatically generated by using eTMQI as the optimization goal. Numerical and subjective experiments demonstrate that eTMQI is a superior objective quality assessment metric for tone mapped images and consistently outperforms.

Index Terms— High dynamic range image, image quality assessment, tone mapping operator, perceptual image processing, structural similarity, statistical naturalness.

I.INTRODUCTION

The luminance of a natural scene often has a high dynamic range(HDR),varying between 10^{-3} to 10^{5}cd/m^{2}. However, a normal digital display only has a low dynamic range (LDR) about10^{2}cd/m^{2}.Tone mapping operators fill in the gap between HDR imaging and visualizing HDR images on standard displays by compressing the dynamic range of HDR images . TMOs provide a useful surrogate for HDR display technology, which is currently still expensive. Regardless of how fast HDR display technology penetrates the market, there will be a strong need to prepare HDR imagery for display on LDR devices.In addition, compressing the dynamic range of an HDR image while preserving its structural detail and natural appearance is by itself an interesting and challenging problem for human and computer vision study.

Most of them were demonstrated on specific examples without being thoroughly evaluated using well-designed and subject-validated image quality assessment (IQA) models. With multiple TMOs at hand, a natural question is: which TMO produces the best quality tone mapped LDR image? This question could possibly be answered by subjective evaluation which is expensive, time consuming, and

perhaps most importantly, can hardly be used to guide automatic optimization procedures.

A promising approach is to develop objective IQA models that can automatically evaluate the performance of TMOs. Traditional objective IQA metrics such as peak signal-to-noise ratio and the structural similarity index (SSIM) assume that the reference and compared images have the same dynamic range; thus they are not applicable in this scenario. Some attempts have been made for objectively assessing the quality of HDR images. The HDR visible difference predictor tries to predict the visible difference between two HDR images with the same dynamic range. A dynamic range independent quality measure focuses on detecting the loss of visible contrast, the amplification of invisible contrast, and the reversal of visible contrast. It produces three corresponding probability maps but does not integrate them into an overall quality score. Recently, a tone mapped image quality index (TMQI) is proposed , which consists of two fundamental building blocks: structural fidelity and statistical naturalness.

II.ITERATIVE TONE MAPPING BY OPTIMIZING TMQI-II

Let **X** and **Y** be the HDR image and the tone mapped LDR image, respectively. TMQI suggests that a high quality tone mapped image should achieve great structural fidelity with respect to the HDR image and high statistical naturalness simultaneously. The computation of TMQI is given by

$$\mathrm{TMQI}(X,Y)= a[S(X,Y)]^{\alpha} + (1-a)[N(Y)]^{\beta} \quad (1)$$

where S and N denote the structural fidelity and statistical naturalness measures, respectively. The parameters α *and* β determine the sensitivities of the two terms, and $0 \leq a \leq 1$ adjusts the relative importance between them. Both S and N are upper bounded by 1 and thus

TMQI is also upper bounded by 1.

As one of the first attempts on quality evaluation of images across dynamic ranges, TMQI achieved remarkable Success, but as will

be shown later, it also has significant limitations. Here, we propose an improved TMQI, namely

TMQI-II, that overcomes the limitations to better correlate with subjective evaluations. Details of TMQI-II will be elaborated later along with the discussions regarding the structural fidelity and Statistical naturalness Assuming TMQI-II to be the quality criterion of tone mapped images, the problem of optimal tone mapping can be formulated as

$$\mathbf{Y}\mathrm{opt}=\arg_{Y}\max \mathrm{TMQI\text{-}II}(\mathbf{X},\mathbf{Y}), \quad (2)$$

where **Y** has a much lower dynamic range than **X**. Solving (2) for **Y**opt is a challenging problem due to the complexity of TMQI-II and the high dimensionality. Therefore, we resort to numerical optimization and propose an iterative approach. Specifically, given any initial image **Y**0, we move it towards the direction in the space of images that improves TMQI-II. To accomplish that, we first improve the structural fidelity S using a gradient ascent method and then enhance the statistical naturalness N by solving a parameter optimization problem for a point

wise intensity transformation. These two steps constitute one iteration and the iterations continue until convergence.

A. Structural Fidelity Update

The structural fidelity of TMQI is computed using a sliding window across the entire image, which results in a quality map that indicates local structural detail preservation. Let **x** and **y** be two image patches within the sliding window in the HDR

$$S_{local}(x;\ y) = \frac{2\tilde{\sigma}x\,\tilde{\sigma}y + C1}{\tilde{\sigma}_x^2 + \tilde{\sigma}_y^2 + C_1} \cdot \frac{2\,\sigma_{xy} + C_2}{\sigma_x + \sigma_y + C_2} \quad (3)$$

where σx , σy and σxy denote the local standard deviations (std) and covariance between the two corresponding patches, respectively. $C1$ and $C2$ are two small positive constants to avoid instability.

It suggests that the HDR and tone mapped image patches should keep the same contrast visibility; otherwise, the contrast of the tone mapped image patch should be penalized, which corresponds to either artificially creating visible contrast or failing to preserve visible contrast. The second component is the same as the structure comparison term in SSIS. The overall structural fidelity measure of the image is computed by averaging all local structural fidelity measures

$$S(X, Y) = \frac{1}{M}\sum_{i=1}^{M} Sloca(X, Y) \quad (4)$$

To assess the visibility of local contrast, the local std σ undergoes a nonlinear function motivated by a contrast sensitivity model

$$\tilde{\sigma}x = \frac{1}{\sqrt{2\pi}\theta_\sigma} \int_{-\infty}^{\sigma} \exp\left[-\frac{(t - T_\sigma)^2}{2\theta_\sigma^2}\right] dt \quad (5)$$

where τ_σ is a threshold determined by the contrast sensitivity function and $\theta\sigma = \tau\sigma$ /3 .The above nonlinear function is limited in accurately assessing the contrast visibility of HDR image patches. First, even a small change in local patch of the HDR image (which may result from the HDR camera noise) may contribute to a significant σ value. When Eq. (5) effectively distinguishes the visible and invisible local contrast in the tone mapped image,it tends to label most patches,either visible or invisible in the HDR image, as contrast visible. Fig. 1 illustrates this phenomenon.

(a)

(b)

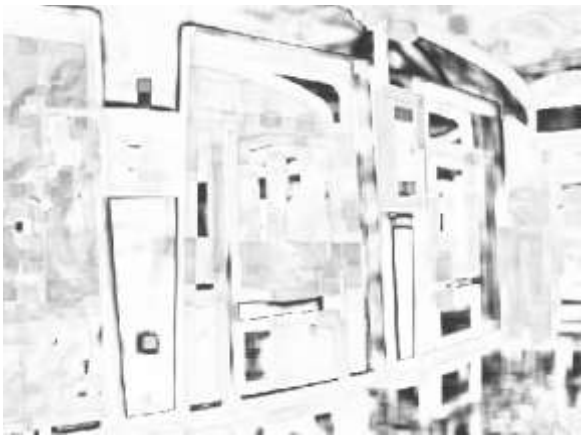

(c)

Fig. 1.Tone mapped "Belgium house" image and its structural fidelity maps. (a) Initial image created by Reinhard's algorith. (b) and (c) Structural fidelity maps generated by TMQI and TMQI-II respectively, where brighter indicates higher structural fidelity.

The homogeneous areas such as the walls and the Wood board in the lower middle part of the image are correctly predicted as contrast invisible in the tone mapped image but mistakenly marked as contrast visible in the HDR image due to over sensitivity to noise. This explains the corresponding dark areas of the structural fidelity map in Fig. 1(b). different local patches in the HDR image may have substantially different

dynamic ranges, which correspond to different thresholds $\tau\sigma$ .In other words, a single $\tau\sigma$ is insufficient to account for the local contrast visibility of the HDR image.The above analysis

suggests that a contrast visibility model adapted to local luminance levels is desired for the HDR image. In particular, we follow and choose σ/μ,namely the coefficient of variation, as an estimate of local contrast in the HDR image, where μ is the local mean. The reason follows directly from the local luminance adaptation that cancels out the scale factors in the numerator and the denominator. Fig. 1(c) shows an example of the structural fidelity map from the modified structural fidelity term, which captures the contrast visibility of the HDR and the tone mapped images more reasonably. Given the modified structural fidelity term, we adopt a gradient ascent algorithm similar to and to improve the structural fidelity of the resulting image $\mathbf{Y}k$ from the k-th iteration. To do that, we compute the gradient of $S(\mathbf{X},\mathbf{Y})$ with respect to $\mathbf{Y}$, denoted by $\nabla\mathbf{Y}S(\mathbf{X},\mathbf{Y})$ and update the image by

$$\hat{Y}_k = Y_k + \lambda \nabla_Y S(X,Y)|_{Y=Y_k} \quad (6)$$

where λ is the step size. To compute the gradient $\nabla\mathbf{Y}S(\mathbf{X},\mathbf{Y})$,we start from the local structural fidelity and rewrite (3) as

$$S_{local} = \frac{A_1 A_2}{B_1 B_2} \quad (7)$$

Where

$$A_1 = 2\tilde{\sigma}_x\tilde{\sigma}_y + C_1 \quad (8)$$

$$B_1 = \tilde{\sigma}_x^2 + \tilde{\sigma}_y^2 + C_2 \quad (9)$$

$$A_2 = \sigma_{xy} + C_2 \quad (10)$$

$$B_2 = \sigma_x\sigma_y + C_2 \quad (11)$$

By treating both image patches as column vectors of length Nw, we have the sample statistics given by

$$\mu_y = \frac{1}{N_w} 1^T y \quad (12)$$

$$\sigma_y^2 = \frac{1}{Nw-1}(y-\mu_y)^T(y-\mu_y) \quad (13)$$

$$\sigma_{xy} = \frac{1}{\mathrm{Nw}-1}(x-\mu_x)^T(y-\mu_y) \quad (14)$$

$$A = \pi r^2$$

where **1** is a *Nw*-vector with all entries equal to 1. The gradient of the local structural fidelity measure with respect to **y** can then be expressed as

$$\nabla_y S_{local} = \frac{(A_1'A_2 + A_2A_1')}{B_1B_2} - \frac{(B_1'B_2 + B_2B_1')A_1A_2}{(B_1B_2)^2} \quad (15)$$

Where

$$A_1' = \nabla_y A_1,\ B_1' = \nabla_y B_1,\ A_2' = \nabla_y A_2,\ B_2' = \nabla_y B_2, \quad (16)$$

Noting That

$$\nabla_y \sigma_y = \frac{1}{N_w \sigma_y}(y-\mu_y) \quad (17)$$

$$\nabla_y \sigma_{xy} = \frac{1}{N_w}(x-\mu_x) \quad (18)$$

We have

$$A_1' = 2\tilde{\sigma}_x \Delta_y \tilde{\sigma}_y = \frac{2\tilde{\sigma}_x}{\sqrt{2\pi}\theta_\sigma} \exp\left[-\frac{(\sigma_y - T_\sigma)^2}{2\theta_\sigma^2}\right] . \Delta_y \sigma_y = \sqrt{\frac{2}{\pi}} \frac{\sigma_x}{N_w \theta_\sigma \sigma_y} \exp\left[-\frac{(\sigma_y - T_\sigma)^2}{2\theta_\sigma^2}\right] . (y-\mu_y) \quad (19)$$

$$B_1' = 2\tilde{\sigma}_y \Delta_y \tilde{\sigma}_y = \sqrt{\frac{2}{\pi}} \frac{\sigma_y}{N_w \theta_\sigma \sigma_y} \exp\left[-\frac{(\sigma_y - T_\sigma)^2}{2\theta_\sigma^2}\right] . (y-\mu_y) \quad (20)$$

$$A_2' = \frac{1}{N_w}(x-\mu_x) \quad (21)$$

$$B_2' = \sigma_x \Delta_y \sigma_y = \frac{\sigma_x}{N_w \sigma_y}(y-\mu_y) \quad (22)$$

Plugging (8), (9), (10), (11), (19), (20), (21) and (22) into (15),we obtain the gradient of local structural fidelity. Finally, we compute the gradient of the overall structural fidelity measure with respect to the tone mapped image **Y** by summing over all the local gradients

$$\Delta_y S(X,Y) = \frac{1}{M}\sum_{i=1}^{M} R_i^T \nabla_y S_{local}(X,Y)|_{X=X_i, Y=Y_i} \quad (23)$$

where $x_i = R_i(X)$ and $y_i = R_i(Y)$ are the i^{th} image patches, R_i is the operator that takes the i^{th} local patch from the image, and R_i^T places the patch back into the corresponding location in the image

B. Statistical Naturalness Update

The statistical naturalness *N* in TMQI is constructed by modeling the histograms of μ and σ of about 3000 natural images by a Gaussian density function *Pm* and a Beta density function *Pd* , respectively. Based on the independence characteristic of image brightness and contrast the two density functions are multiplied to obtain the overall statistical naturalness measure

$$\mathrm{N(Y)} = \frac{1}{K} P_m P_d \quad (24)$$

where *K* is a normalization factor.

The above statistical naturalness model has two limitations.First, *Pm* and *Pd* are assumed to be completely independent of image content, which is an over simplification. The model suggests that to be highly statistically natural, the tone mapped image of dynamic range [0, 255] should have μ around 116 and σ around 65 which correspond to the peaks in *Pm* and *Pd* ,respectively .However, each image may have a different μ and σ to look perfectly natural depending on its content.Second, the model is derived from high quality images,with no information about what an unnatural image may look like.Here we

propose an image dependent statistical naturalness model based on a subjective experiment to better quantify the unnaturalness of tone mapped images. First, we estimate the overall luminance and global contrast directly from the HDR image, denoted by μe and σe, respectively. The quantity is computed by

$$L_x = \exp\left(\frac{1}{|X|}\sum_{i,j}\log(\in + X(i,j))\right) \quad (25)$$

where $\mathbf{X}(i, j)$ is the luminance of the HDR image at location (i, j), $|\mathbf{X}|$ is the cardinality and is a small positive constant to avoid instability. Next,
the luminance is scaled by

$$X^s(\mathrm{i},\mathrm{j}) = \frac{K}{L_x} X(i,j) \quad (26)$$

where k is a luminance level related quantity typically set between 0.09 and 0.36 for an HDR image with normal luminance level [3]. μe and σe are then estimated by

$$\mu_e = \frac{L}{|X|}\left(\sum_{i,j}\frac{X^s(\mathrm{i},\mathrm{j})}{1+X^s(\mathrm{i},\mathrm{j})}\right) \quad (27)$$

And

$$\sigma_e = \frac{1}{|X|-1}\left(\sum_{i,j}\frac{X^s(\mathrm{i},\mathrm{j})}{1+X^s(\mathrm{i},\mathrm{j})}L - \mu_e\right) \quad (28)$$

where L is the dynamic range of the tone mapped image.Here, the high luminance is further compressed by a factor of $\mathbf{X}s$. This inevitably causes detail loss in high luminance areas.
Nevertheless, our goal here is to roughly estimate μe and σe that are relevant to a natural appearance
of the tone mapped image. This estimation of initial luminance level of the LDR image is closely related to previous works μ_e and σ_e are only rough estimates of the desired μ and σ values.

For each LDR image, there should be certain ranges of μ and σ values surrounding μe and σ_e,within which the naturalness of the image is not degraded. To verify this and to provide a quantitative model, we conducted a subjective experiment, in which observers were asked to gradually decrease and then increase μ of the test
LDR images until they saw significant degradation in naturalness. A lower bound μ_l and a upper bound μ_r for each LDR image were thus recorded. The same procedure is used to obtain a lower std bound σ_l and a upper std bound σ_r for each LDR image. We selected 60 natural LDR images from
the LIVE database with different μ and σ values that cover diverse natural contents. Perhaps the most interesting finding in this experiment is when μ of an image is relatively small, μ_r -μ is much large than μ - μ_l . By contrast, the situation is reversed when μ of an image is large. In words, the acceptable luminance changes without significantly tampering an image's visual naturalness saturate at both small and large luminance levels. Similarly,σ_l and σ_r of a test LDR image can also be fitted by two linear models using σ as the predictor. Based on the method described above, given an HDR image,we first estimate μ_e and σ_e and then predict μ_l , μ_r , σ_l and σ_r of the tone mapped image. The μ and σ values of a natural looking tone mapped image should at least fall in $[\mu_l,\mu_r]$ and $[\sigma_l, \sigma_r]$, and if possible, close to μ_e and σ_e. We quantify the drop from μ_e and σ_e to their lower and upper

bounds using Gaussian cumulative distribution
unctions (CDF). Specifically,the likelihood of a tone mapped image to be natural given its mean μ

$$P_m = \begin{cases} \frac{1}{\sqrt{2\pi}\theta_1} \int_{-\infty}^{\mu} \exp[-\frac{(t-T_1)^2}{2\theta_1^2}]\,dt & \mu \le \mu_e \\ \frac{1}{\sqrt{2\pi}\theta_2} \int_{-\infty}^{2\mu_r-\mu} \exp[-\frac{(t-T_2)^2}{2\theta_2^2}]\,dt & \mu > \mu_e \end{cases} \quad (29)$$

where $\tau 1$ and $\theta 1$ are uniquely determined by two
points $(\mu l\ ,\ 0.01)$ and $(\mu e,\ 1)$ on the Gaussian CDF
curve. Correspondingly,$\tau 2$ and $\theta 2$ are uniquely determined by two points $(\mu r\ ,\ 0.01)$ and $(\mu e,\ 1)$ on the Gaussian CDF curve.

$$P_d = \begin{cases} \frac{1}{\sqrt{2\pi}\theta_3} \int_{-\infty}^{\sigma} \exp[-\frac{(t-T_1)^2}{2\theta_3^2}]\,dt & \sigma \le \sigma_e \\ \frac{1}{\sqrt{2\pi}\theta_4} \int_{-\infty}^{2\sigma_r-\sigma} \exp[-\frac{(t-T_2)^2}{2\theta_4^2}]\,dt & \sigma > \sigma_e \end{cases} \quad (30)$$

where $\tau 3$ and $\theta 3$ are uniquely determined by two
oints $(\sigma l\ ,\ 0.01)$ and $(\sigma e,\ 1)$ on the Gaussian CDF curve,and $\tau 4$ and $\theta 4$ are uniquely determined by two points $(\sigma r\ ,\ 0.01)$ and $(\sigma e,\ 1)$ on the Gaussian CDF curve. The models give heavy penalty when $|\mu - \mu e|$ or $|\sigma - \sigma e|$ is large.Similar to Eq. (24), assuming the independence of image luminance and contrast, we multiply these two quantities and obtain the overall statistical naturalness model

$$N(\mathbf{X},\mathbf{Y}) = PmPd \quad (31)$$

ince $0 \le Pm, Pd \le 1$, N also lies in [0, 1]. The superiority of the modified statistical naturalness term over that in TMQI is verified by improved correlation with respect to subjective evaluations .

To continue with the iterative optimization procedure upon structural fidelity update, we start intermediate image $\hat{\mathbf{Y}}k$ in Eq. (6) and improve the

statistical naturalness to achieve $\mathbf{Y}k+1$ through a three-segment equipartition monotonic
piecewise linear function

$$y_{k+1}^i = \begin{cases} (3/L)a\tilde{y}_k^i & 0 \le \tilde{y}_k^i \le L/3 \\ (3/L)(b-a)a\tilde{y}_k^i + (2a-b) & L/3 \le \tilde{y}_k^i \le 2L/3 \\ (3/L)(L-b)\tilde{y}_k^i + (3b-2L) & 2L/3 \le \tilde{y}_k^i \le L \end{cases} \quad (32)$$

$$\mu_{k+1}^e = \tilde{\mu}_k + (\lambda_m - \tilde{\mu}_k) \quad (33)$$

$$\sigma_{k+1}^e = \tilde{\sigma}_k + (\lambda_d - \tilde{\sigma}_k)$$

where $\tilde{\mu}_k$ and $\tilde{\sigma}_k$ are the mean and std of $\hat{\mathbf{Y}}_k$, respectively.λ_m and λ_d are step sizes that control
the updating speed.

$$\text{TMQI-II}(\mathbf{X},\mathbf{Y}) = a[S(\mathbf{X},\mathbf{Y})]^{\alpha} + (1-a)[N(\mathbf{X},\mathbf{Y})]^{\beta}, \quad (35)$$

where both S and N measures have been improved upon those in TMQI.

III. EXPERIMENTAL RESULTS

To fully demonstrate the potentials of the proposed iterative algorithm, we select a wide range of HDR images, containing both indoor and outdoor scenes, human and static objects. It can be observed that the structural fidelity map is very effective at detecting the missing structures the proposed algorithm successfully recovers such details after a sufficient number of iterations. The improvement of structural detail is also well reflected by the structural fidelity. We apply the proposed iterative algorithm but using statistical naturalness updates only. With the iterations, the overall brightness and contrast of the image are significantly improved,

leading to a more visually appealing and natural-looking image.

The Table. 1. represents the Mean squre value and Peak signal to noise ratio for the indoor images .Here,we can observe that Peak signal to noise ratio is increasing in each iteration level possible.

The Fig. 2.(a,b,c,d,e,f) shows the input images at different contrast levels which are undergoing process of images quality assessment Through our Tone mapped quality operators we converted high dynamic range image to low dynamic image with the high Structural fidelity and statistical naturalness as shown below Fig. 3.

Table 1. Comparison of MSE and PSNR values at different iteration levels for indoor images

S.NO	MSE	PSNR
1	34.97	32.7278214 dB
2	56.46	30.6476407 dB
3	80.15	29.1258022 dB

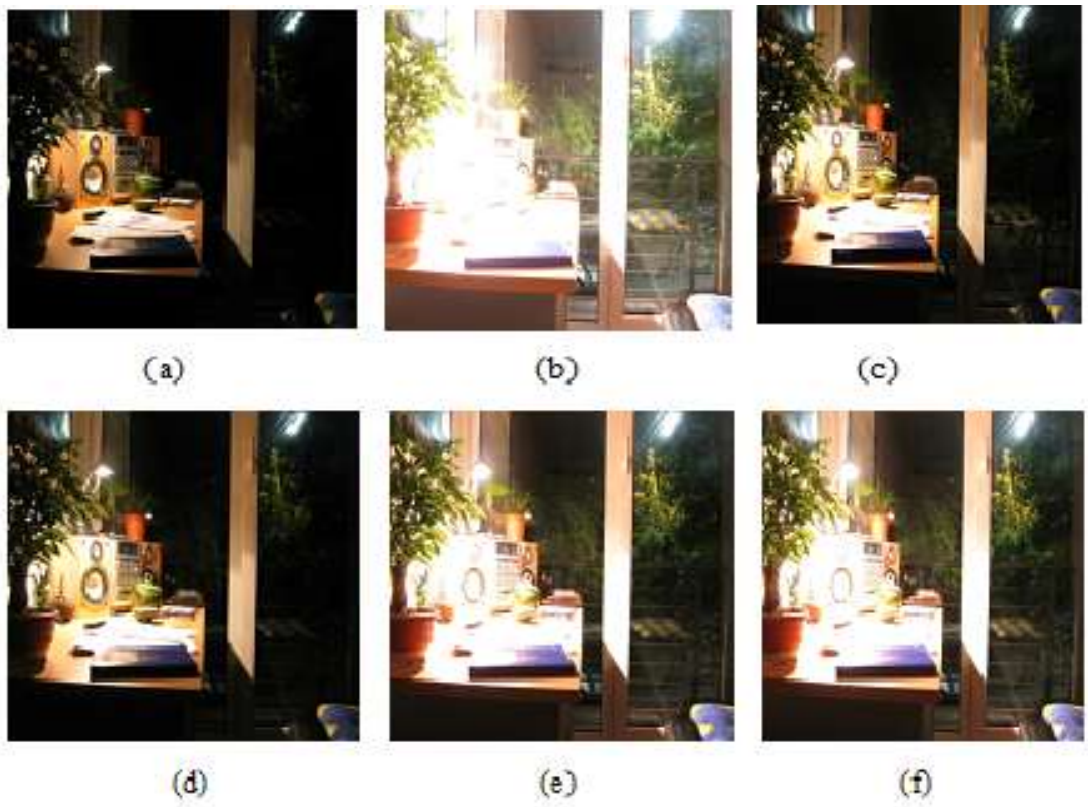

Fig. 2. (a,b,c,d,e,f) Input images(Indoor) at different contrast levels

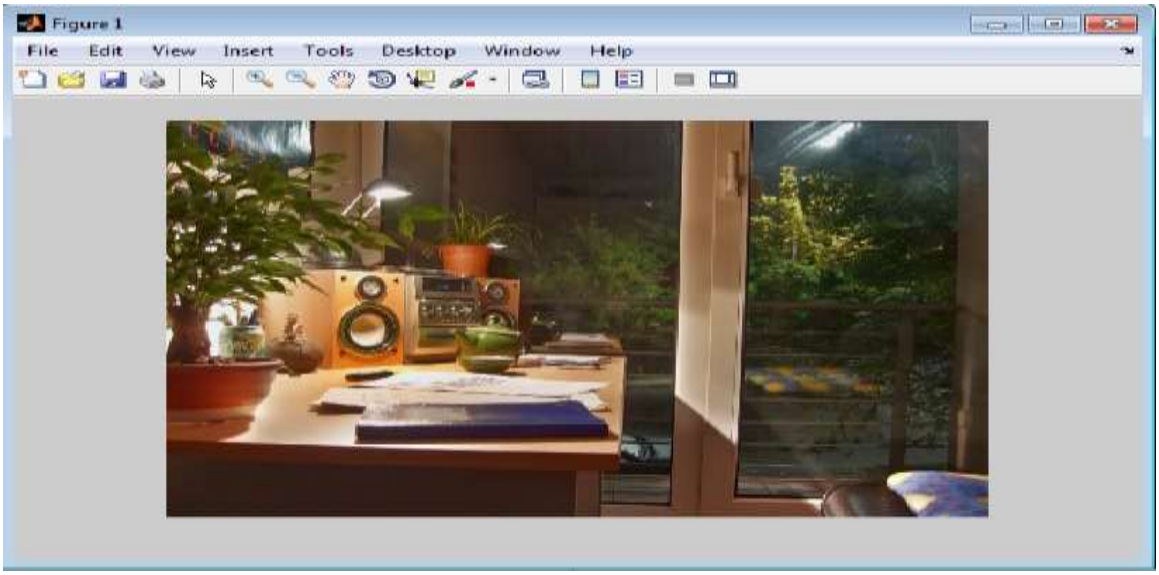

Fig. 3. LDR output image(Indoor) generated by TMQI-II Method

REFERENCES

[1] B. A. Wandell, *Foundations of Vision*. Sunderland, MA, USA: Sinauer Associates.

[2] E. Reinhard, W. Heidrich, P. Debevec, S. Pattanaik, G. Ward, and K. Myszkowski, *High Dynamic Range Imaging: Acquisition, Display, and Image-Based Lighting*. San Mateo, CA, USA: Morgan Kaufmann,2010.

[3] E. Reinhard, M. Stark, P. Shirley, and J. Ferwerda, "Photographic tone reproduction for digital images," *ACM Trans. Graph.*, vol. 21, no. 3, pp. 267–276, 2002.

[4] F. Drago, K. Myszkowski, T. Annen, and N. Chiba, "Adaptive loga- rithmic mapping for displaying high contrast scenes," *Comput. Graph. Forum*, vol. 22, no. 3, pp. 419–426.

[5] Q. Shan, J. Jia, and M. S. Brown, "Globally optimized linear windowed tone mapping," *IEEE Trans. Vis. Comput. Graphics*, vol. 16, no. 4, pp. 663–675, Jul./Aug. 2010.

[6] S. Ferradans, M. Bertalmio, E. Provenzi, and V. Caselles, "An analysis of visual adaptation and contrast perception for tone mapping," *IEEE Trans. Pattern Anal. Mach. Intell.*, vol. 33, no. 10, pp. 2002–2012, Oct. 2011.

[7] B. Gu, W. Li, M. Zhu, and M. Wang, "Local edge-preserving multiscale decomposition for high dynamic range image tone mapping," *IEEE Trans. Image Process.*, vol. 22, no. 1, pp. 70–79, Jan. 2013.

[8] H. Yeganeh and Z. Wang, "High dynamic range image tone mapping by maximizing a structural fidelity measure," in *Proc. IEEE Int. Conf. Acoust., Speech Signal Process.*, May 2013, pp. 1879–1883.

[9] K. Ma, H. Yeganeh, K. Zeng, and Z. Wang, "High dynamic range image tone mapping by optimizing tone mapped

image quality index," in *Proc.IEEE Int. Conf. Multimedia Expo.*

[10] F. Drago, W. L. Martens, K. Myszkowski, and H.-P. Seidel, "Perceptual evaluation of tone mapping operators," in *Proc. ACM SIGGRAPH Sketches Appl.*, 2003, p. 1.

AUTHOR'S BIOGRAPHY

V.Phanibhushan, Graduate in Electronics & Communication Engg. from institution of electronics and telecommunication engineers, Newdelhi in the year 1999. Later Worked as Asst.Professor in the Dept.of ECE, PBRVITS, Kavali. Obtained Master Degree in Digital Systems & Computer Electronics from JNTU, Anantapur in 2009. Currently working as Associate professor in the Dept.of ECE, PBRVITS, Kavali and has teaching experience of 15 years. His area of interest includes Digital electronics,Microprocessors & Microcontrollers, Digital Image processing & Digital IC Applications.

B.Sravani has received his B.Tech degree in Electronics and Communication Engineering from JNTUA, Anatapuramu in 2014. She is now pursuing the M.Tech degree at PBR Visvodaya Institute of Technology and Science, Kavali, Andhra Pradesh, India. Her areas of research include digital image processing.